NANO LETTERS

Letter

pubs.acs.org/NanoLett

Dissecting Contact Mechanics from Quantum Interference in Single-Molecule Junctions of Stilbene Derivatives

Sriharsha V. Aradhya,[†,∥] Jeffrey S. Meisner,[‡,∥] Markrete Krikorian,[‡] Seokhoon Ahn,[‡] Radha Parameswaran,[§] Michael L. Steigerwald,[‡] Colin Nuckolls,*[,‡] and Latha Venkataraman*[,†]

[†]Department of Applied Physics and Applied Mathematics and [‡]Department of Chemistry, Columbia University, New York, New York, United States

[§]Departments of Chemistry and Physics, Barnard College, New York, New York, United States

Supporting Information

ABSTRACT: Electronic factors in molecules such as quantum interference and cross-conjugation can lead to dramatic modulation and suppression of conductance in single-molecule junctions. Probing such effects at the single-molecule level requires simultaneous measurements of independent junction properties, as conductance alone cannot provide conclusive evidence of junction formation for molecules with low conductivity. Here, we compare the mechanics of the conducting para-terminated 4,4′-di-(methylthio)stilbene and moderately conducting 1,2-bis(4-(methylthio)phenyl)ethane to that of insulating meta-terminated 3,3′-di(methylthio)stilbene single-molecule junctions. We simultaneously measure force and conductance across single-molecule junctions and use force signatures to obtain independent evidence of junction formation and rupture in the meta-linked cross-conjugated molecule even when no clear low-bias conductance is measured. By separately quantifying conductance and mechanics, we identify the formation of atypical 3,3′-di(methylthio)stilbene molecular junctions that are mechanically stable but electronically decoupled. While theoretical studies have envisaged many plausible systems where quantum interference might be observed, our experiments provide the first direct quantitative study of the interplay between contact mechanics and the distinctively quantum mechanical nature of electronic transport in single-molecule junctions.

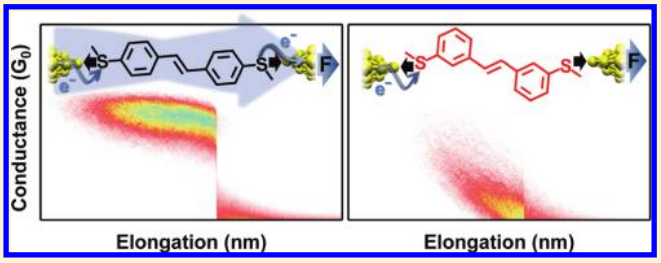

KEYWORDS: *Single molecule electronics, contact mechanics, rupture force, quantum interference, donor−acceptor interaction*

Understanding and controlling the electronic properties of molecular wires is fundamentally important for molecular electronics.[1,2] The scanning tunneling microscope (STM) based break junction approach gives a deep insight into the structure-conductance relationship in single-molecule junctions because it provides a statistical interpretation over an ensemble of measurements.[3−5] However, in these studies only one physical property, the junction conductance, is measured. This limits the interpretation of the results in junctions where the conductance is either very small or ill-defined. Theory predicts that there will be large modulations in single molecule conductance for systems exhibiting quantum interference, such as variously substituted aromatic molecules and cross-conjugated molecular wires.[6−12] For example, theoretical calculations have predicted that a benzene ring bound to metal electrodes with linker groups at the 1 and 3 positions (meta to each other) should have a conductance that is 5 orders of magnitude lower than that of a 1,4-linked benzene.[6] To determine, from low-bias conductance measurements alone, whether such effects are present is difficult because the conductance of the meta-substituted molecules is often below the experimental noise limit of the instruments. At high biases, nonequilibrium effects, junction heating, and inelastic processes cannot be ruled out.[13−15] Furthermore, a statistical approach is needed to demonstrate the robustness of interference phenomenon by rigorously accounting for experimental details such as junction formation probability, binding strength, junction-to-junction variation and junction structure.

In this manuscript, we overcome these critical challenges by simultaneously measuring force and conductance across single molecule junctions using a conducting atomic force microscope setup.[16,17] We study three molecular backbones: 4,4′-di-(methylthio)stilbene (**1**), 1,2-bis(4-(methylthio)phenyl)ethane (**2**), and 3,3′-di(methylthio)stilbene (**3**). These molecules are chosen since the longer stilbene backbones, rather than benzene backbones discussed above, form molecular junctions more frequently and the thiomethyl (SMe) terminal groups provide reliable mechanical and electrical contact to the Au electrodes.[18,19] We exploit the high binding probabilities and reliable contact properties to acquire and analyze large data sets comprised of thousands of individual junctions to probe the robustness of interference effects, in each case. The para-positioned linker groups in **1** effectively couple across the π-

Received: December 29, 2011
Revised: February 13, 2012
Published: February 21, 2012

system and provide a conducting single-molecule junction. In **2**, the mechanical linkages between the metal and the molecule are the same as in **1**, but conjugation is broken due to the saturated bridge, which results in lower junction conductance. In **3**, the mechanical linkers are moved to the meta-position but the conjugated bridge is retained, as in **1**. There is no measurable single molecule conductance feature in **3**. We use the simultaneously measured force data to independently obtain signatures of junction formation and rupture. We quantitatively determine the elongation length and rupture force for each of the three molecules, irrespective of their conductance. In contrast to the conductance, we find that the rupture force is insensitive to the linker group placement. We are able to demonstrate, for the first time, that the meta-substituted **3** forms mechanically stable Au−molecule−Au junctions but does not show a measurable conductance, and theoretical calculations point to quantum mechanical interference as the origin of this behavior. These measurements enable us not only to investigate junctions of nonconducting molecules, but more generally allow us to deconvolute electronic effects from mechanical evolution in single-molecule junctions.

Simultaneous measurements of single-molecule conductance and force are carried out using a custom-built conductive atomic force microscope (AFM), which has been described in detail previously.[17] Molecular junctions are formed between an Au-coated AFM cantilever and an Au-on-mica substrate schematically represented in Figure 1a. Conductance is

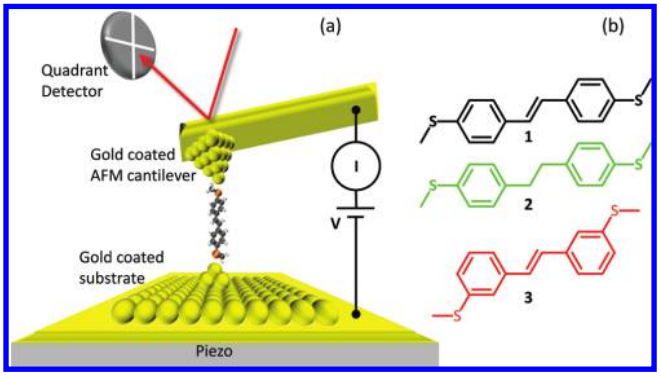

Figure 1. (a) Schematic of AFM apparatus and (b) chemical structures of molecules **1**−**3**.

determined by measuring current through the junction at an applied bias of 75 mV. Simultaneous measurements of cantilever deflection relate to the force applied across the junction. The AFM is operated in ambient conditions at room temperature. Dilute solutions (0.1 mM) of the target molecules (**1**−**3**, Figure 1b) in 1,2,4-trichlorobenzene are deposited on the substrate. For each measurement, the tip is brought into contact with the substrate until a conductance greater than 5 G_0 ($G_0 = 2e^2/h$, the quantum of conductance) is achieved and then retracted at a constant velocity of 18 nm/s while both conductance and cantilever deflection are continuously recorded. During this elongation, the Au contact thins down to a single atom point contact, clearly identified by a conductance plateau of 1 G_0. In the absence of molecules the Au contact ruptures to a broken junction when elongated further. However, in a solution of molecules, molecular junctions are frequently formed after the rupture of the 1 G_0 plateau.

Figure 2 displays simultaneously measured force and conductance traces obtained while breaking Au point contacts

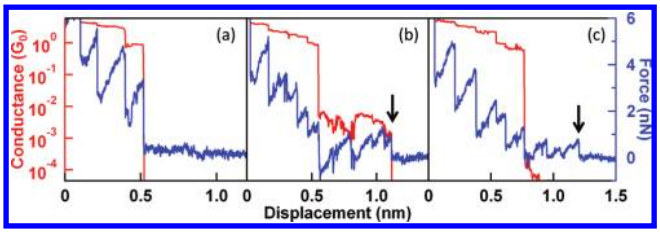

Figure 2. Sample traces of simultaneously measured conductance (red, left axis) and force (blue, right axis) for (a) Au−Au junctions (b) Au−**1**−Au and (c) Au−**3**−Au single molecule junctions. Downward arrows indicate the final force event identifying junction rupture.

without molecules (Figure 2a) or with **1** and **3** (Figure 2 panels b and c, respectively). We see a stepwise decrease in conductance (red) while the simultaneously measured force (blue) has a characteristic sawtooth pattern with alternating linear ramps (elastic loading) and abrupt drops (structural rearrangement or bond rupture) in force.[17,20] After the rupture of the Au single-atom contact in the absence of molecules (identified by its characteristic 1 G_0 conductance plateau), no further features are seen in either conductance or force. The conductance drops below the measurable level (~10^{-5} G_0), and the force stays constant because there is no more a load on the cantilever, as seen in Figure 2a. When an Au point contact is broken in the presence of **1** or **2**, a single-molecule junction with a characteristic conductance feature is formed ~90% of the time.[18,19] This additional plateau is seen in the conductance traces immediately following the rupture of the Au contact, as illustrated in Figure 2b (red trace) for an individual measurement with **1**. The simultaneously acquired force traces (blue) also show additional sawtooth features. In this trace, we see that the 1 G_0 ruptures at ~0.5 nm along the displacement axis and the molecular junction ruptures after an additional elongation of about 0.6 nm. Once this molecular junction has ruptured, no more conductance or force features are seen in measurements with **1** or **2**. In contrast, measurements with **3** do not exhibit any well-defined conductance plateau, however a majority of the measured traces show multiple force features after the rupture of the Au-contact as illustrated in Figure 2c. Such force features are similar in magnitude to those seen in measurements of **1** and **2**.

For each molecule (**1**−**3**), we analyze 7000 simultaneously measured conductance and force traces using an automated algorithm detailed in the Supporting Information document. We use these large data sets to obtain statistically significant information because the atomic-scale structure varies from junction to junction. We begin by locating the displacement when the Au point contact ruptures in the conductance traces. This is the point in the trace when conductance drops below 1 G_0. Focusing on the simultanesouly acquired force trace, we analyze a 1 nm long segment of this trace (~S−S distance for the three molecules) beyond the 1 G_0 rupture point to locate the final junction rupture event, that is, the last abrupt force drop. The distance between the 1 G_0 rupture location and this final force event defines the molecular junction elongation length. For conducting molecules (Figure 2b), we observe that molecular junctions form immediately after the rupture of the Au point contacts and therefore junction elongation length is equivalent to the conductance plateau length, which has been

dx.doi.org/10.1021/nl2045815 | *Nano Lett.* 2012, 12, 1643−1647

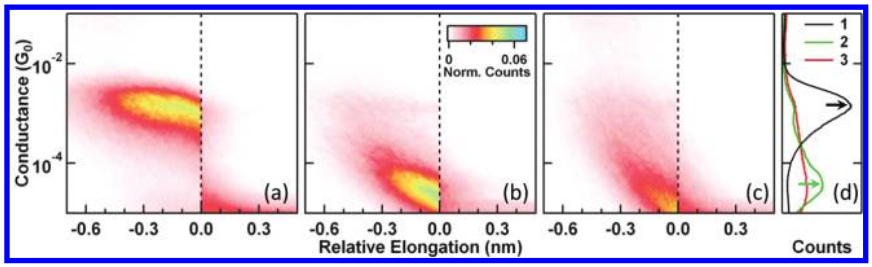

Figure 3. Displacement-preserving 2D conductance histograms (a, b, c) for **1**, **2**, and **3**, respectively, and profiles of conductance before rupture (d). The histograms represent more than 85% of the 7000 measured traces that show a significant force event beyond Au rupture in each case. The abrupt jump in conductance at the displacement origin (dashed vertical lines provided as a visual guide) for **1** and **2** shows that bond rupture coincides with conductance drops. Arrows indicate the most frequently measured conductance value from the conductance profiles of **1** and **2**.

used in previous studies to characterize single-molecule junction mechanics.[16,18,21] It is important to note that we are able to identify molecular junction rupture events through force data and do not require a well-defined conductance plateau to obtain the elongation length.

Two-dimensional conductance and force histograms are now generated using the location of the final force event as the origin along the displacement axis.[18] For conductance, individual traces are offset laterally such that the rupture location is the origin of the displacement axis. The 2D conductance histograms have linear bins along the displacement axis (x-axis, 500 bins/nm) and logarithmic bins along the conductance axis (y-axis, 200 bins/decade).[22] For force data, individual traces are offset both laterally as above and vertically such that the force value at the origin is zero. The 2D force histograms have linear bins along displacement (x, 500 bins/nm) and force (y, 12.5 bins/nN) axes. Every vertical section of this 2D force histogram is fit with a Gaussian and its peak is used to determine a statistically averaged force profile for the entire data set.[17] Since there is no selection based on conductance, every trace with a significant force event after Au rupture (>85% of measured traces in each case) is analyzed.

In Figure 2b, we display a sample force and conductance measurement with **1**. We see a clear conductance plateau after the rupture of Au point contacts. The simultaneously acquired force traces shows several sawtooth features indicating multiple structural changes in the junction, ultimately rupturing after ~0.6 nm of elongation.[23] The final force event (downward arrow in Figure 2b) occurs at exactly the same displacement as the conductance drop. Figure 3a shows the 2D conductance histogram for **1** representing 6788 of the 7000 individual traces for which a significant force event was found after 1 G_0 rupture. Although only force data was used to identify and set the zero displacement at the molecular junction rupture point, we observe that the conductance also drops sharply to the instrument noise level at zero-displacement, demonstrating the reliability of this force-based alignment procedure. A conductance profile of this histogram shows a clear peak at 1.3×10^{-3} G_0 (Figure 3d, black trace), which compares well with the 1D conductance histograms created from all the measured traces (see Supporting Information). We see that the para-linked molecule **1** forms junctions with relatively high, well-defined conductance, as observed for other fully conjugated molecular wires. The 2D force histogram created from the simultaneously acquired force traces is shown in Figure 4, along with the statistically averaged force profile. This force profile shows an abrupt drop of 0.5 nN at zero displacement, corresponding to the force required to rupture this junction.[17]

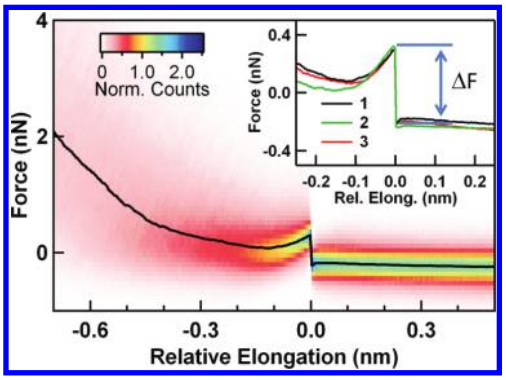

Figure 4. The 2D force histogram for molecule **1** with the averaged force profile overlaid. (Inset) Statistically averaged force profiles for molecular junctions of **1**, **2**, and **3** in black, green, and red, respectively.

Molecule **2** shows similar behavior in conductance and force. The 2D conductance histogram (Figure 3b, from 6332 traces) shows a clear conductance feature at a significantly lower value of 3.2×10^{-5} G_0. This result is intuitively understood as arising from the lowered communication between the aromatic rings due to the ethane bridge at the center, even though the para-positions of the linkers is identical to **1**. The 2D force histogram created from the simultaneously acquired force traces is shown in Supporting Information Figure S3a. From the statistically averaged force profile (inset, Figure 4, green trace), we find that these junctions also rupture at a force of 0.5 nN and show a loading and rupture behavior similar to **1**.

Qualitatively different behavior is found in junctions of **3**. We do not see clear conductance plateaus in individual traces, as shown in Figure 2c. Individual force traces, however, do show sawtooth signatures typical of junction structure evolution and bond rupture and are analogus to force measurements of **1** and **2**. This is representative of the loading and rupture event of the molecular junction in individual traces. The 2D conductance histogram (Figure 3c), constructed from all traces that show a clear bond rupture event in the force data, shows a broad conductance feature slightly above the noise level as seen in the profile in Figure 3d (red trace). This can be ascribed to the small, but nonzero contribution to conductance from the sigma channel, through-space tunneling between the electrodes and possibly dispersive interactions between the molecular π-orbitals and the Au electrodes.[9,24] The 2D force histogram for this molecule is shown in Supporting Information Figure S3b. The averaged force profile centered at the rupture event generated from 5965 traces is shown in the inset of Figure 4 (red trace). Clearly, there are a statistically significant number of traces that have rupture events after the G_0 plateau, a fraction

dx.doi.org/10.1021/nl2045815 | Nano Lett. 2012, 12, 1643–1647

similar to **1** and **2**, which could not be identified by conductance data alone. The bond rupture force for these junctions is also 0.5 nN. Therefore, we conclude that single-molecule junctions of **3** are formed but do not show clear conductance plateaus and have a significantly lower conductance, confirming the theoretical predictions of a low conductance due to interference effects. It is important to note that the character of the conductance we observe for **3** is qualitatively very different from that seen in **1** or **2**, as is further evidenced in the conventional linear and log binned 1D conductance histograms shown in Supporting Information Figure S4.

Taken together, the force profiles for **1**, **2**, and **3** illustrate that bond rupture forces are approximately the same for all three molecular junctions, independent of the linker position. The rupture force depends on the specific interaction of the Au-SMe donor–acceptor bond in each molecule, and the apparent insensitivity of the rupture force to the linker position, within our experimental resolution, can be explained by the similar local structure near the Au-SMe bonds for **1**–**3**.

The independent analysis of force and conductance allows us to study the mechanical aspects of junction evolution even in the absence of conductance plateaus. In particular, the amount of elongation sustained by the junction before rupture, the junction elongation length, gives information about the geometry of the Au–molecule–Au junction. In general, the molecule in the junction can sample multiple binding sites during elongation before achieving the idealized vertical Au–molecule–Au junction geometry.[18] The junction elongation length scales with the molecular S–S distance but is smaller than the molecule length, because of a nonzero gap that is opened when the Au point contact is broken.[22] Histograms of elongation lengths are constructed from individual traces and have a Gaussian distribution (Supporting Information Figure S5). The peak values obtained from these distributions for **1**–**3** are presented in Table 1. The plateau lengths of **1** and **3** are in accordance with their respective S–S distances. However, a relatively smaller plateau length is observed for **2**. This could be due to nonplanar configurations accessible to the ethane bridge in **2**, which are not allowed in either **1** or **3** due to the central C=C double bond. These measured elongation lengths give us further confirmation of the junction formation, independent of conductance.[3,25]

Table 1. Conductance, Elongation Length, and Rupture Force for Single Molecule Junctions with Molecules 1–3

	experimental measurements			DFT
molecule	conductance (G_0)	elongation length (nm)	rupture force (nN)	S–S distance (nm)[a]
1	1.3×10^{-3}	0.42	0.5	1.31
2	3.2×10^{-5}	0.32	0.5	1.29
3[b]		0.31	0.5	1.17

[a]B3LYP/6-31G** level of theory. [b]Nonconductive molecule did not show well-defined peak in conductance profiles.

Having established the similar mechanical stability for **1**–**3**, we are able to make direct comparisons between the chemical structures and the corresponding conductances. We can unambiguously conclude that **2** is less conducting than **1** due to broken conjugation, while **3** forms mechanically stable yet electrically insulating junctions. Molecular backbones **1** and **3** are essentially planar structures with all sp^2-carbon atoms and with similar molecular lengths; however, the meta-positioned linker groups effectively turn off the conductance.

To better understand these results, we have examined the electronic structures of the organic molecules bonded to an Au dimer (which represents one of the Au electrodes) through an Au–S donor–acceptor bond. We use a dimer of Au atoms to avoid complications attendant to the unpaired spin occupying the valence 6s orbital of a single Au atom. We attach the candidate organic molecule to just one "electrode" in order to appreciate what the second electrode sees as it encounters the metal-bound organic. In effect, this is a simplified model for the chemical state of the system prior to the charge transfer. We performed DFT calculations of the electronic structures of these model systems at the B3LYP/6-31G** level.[26] The highest occupied molecular orbital (HOMO) from the geometry-optimized structures, Au_2-**1**, Au_2-**2**, and Au_2-**3**, are shown in Figure 5. The HOMO of **1** extends across the entire π-space of the molecule in contrast to that of **2** and **3**. Significantly, in **1** the HOMO connects both the terminal sulfur atoms and provides a clear electronic conduit between the sulfur groups. In contrast, in **2** one side of the molecule does not communicate with the other, which is a direct result of the saturated ethane bridge. In addition, rotation around these sp^3-carbons increases the conformational freedom in the molecular junction. Therefore, a broad peak is expected in the conductance histograms without retarding the rupture force. In **3**, we observe that although the HOMO extends across the bridge, it does not have significant amplitude on the sulfur atom at the meta-position. This finding is consistent with observations from various related approaches, such as organic reaction kinetics,[27,28] Hammett coefficients,[29] and even classic organic arrow-pushing conventions, which predict a node at the

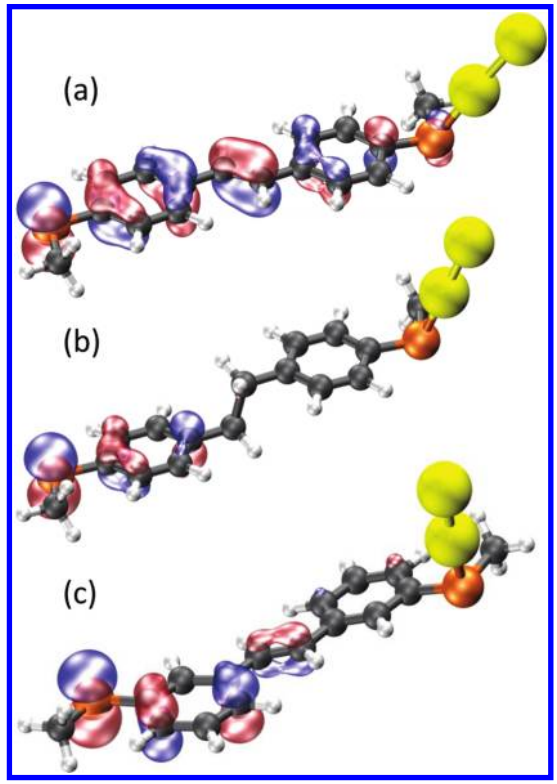

Figure 5. DFT optimized structures and isosurface plots of the HOMO of (a) Au_2-**1**, (b) Au_2-**2**, and (c) Au_2-**3**.

dx.doi.org/10.1021/nl2045815 | *Nano Lett.* 2012, 12, 1643–1647

meta-position.[30] For direct experimental evidence, Daub and co-workers electrochemically quantified the charge-transport kinetics between meta- and para-(styryl)stilbenes.[31] However, this area has recently received more theoretical attention due to the possibility of studying these effects at the single-molecule level.[6−12]

In summary, single-molecule junctions of stilbene derivates with para and meta-linked stilbenes have been formed using a conducting-AFM approach that allows for measurements of single-molecule mechanics through force, independent of conductance. We have found that despite great differences in their conductance values, each molecule assembles into single-molecule junctions that are mechanically stable. Our results show that both para- and meta-linkers provide similar mechanical stability to the junctions yet radically change the conductance. For these reasons the para-linker groups behave as typical electro-mechano contacts, while meta-linkers disrupt the conduction acting primarily as mechanical contacts. By quantitatively accounting for the contact mechanics, these results represent the first direct proof that quantum interference is an inherent property arising from the molecular structure and is not quenched by microscopic junction-to-junction variations. This two-property measurement capability extends our understanding of single-molecule junction properties to such low-conductive and insulating systems as simple molecular connectors and dielectrics materials. Moreover, this approach provides a means to design and study new molecular switches and devices that utilize quantum interference.

■ ASSOCIATED CONTENT

Supporting Information

Synthetic details and characterization data for compounds **1**−**3**; details of experimental setup and analysis methods. This material is available free of charge via the Internet at http://pubs.acs.org.

■ AUTHOR INFORMATION

Corresponding Author

*E-mail: (L.V.) lv2117@columbia.edu; (C.N.) cn37@columbia.edu.

Author Contributions

‖These authors contributed equally to this study.

Notes

The authors declare no competing financial interest.

■ ACKNOWLEDGMENTS

This work has been supported in part by the NSF Career Award (CHE-07-44185) and the Packard Foundation. This research was also funded by the National Science Foundation Center for Chemical Innovation (CCI Phase 1 - Award Number CHE-09-43957).

■ REFERENCES

(1) Nitzan, A.; Ratner, M. A. *Science* **2003**, *300* (5624), 1384−1389.
(2) Joachim, C.; Gimzewski, J. K.; Aviram, A. *Nature* **2000**, *408* (6812), 541−548.
(3) Xu, B.; Tao, N. J. *Science* **2003**, *301* (5637), 1221−1223.
(4) Venkataraman, L.; Klare, J. E.; Tam, I. W.; Nuckolls, C.; Hybertsen, M. S.; Steigerwald, M. L. *Nano Lett.* **2006**, *6* (3), 458−462.
(5) Li, C.; Pobelov, I.; Wandlowski, T.; Bagrets, A.; Arnold, A.; Evers, F. *J. Am. Chem. Soc.* **2007**, *130* (1), 318−326.
(6) Solomon, G. C.; Andrews, D. Q.; Hansen, T.; Goldsmith, R. H.; Wasielewski, M. R.; Duyne, R. P. V; Ratner, M. A. *J. Chem. Phys.* **2008**, *129* (5), 054701.
(7) Markussen, T.; Stadler, R.; Thygesen, K. S. *Nano Lett.* **2010**, *10* (10), 4260−4265.
(8) Tsuji, Y.; Staykov, A.; Yoshizawa, K. *J. Am. Chem. Soc.* **2011**, *133* (15), 5955−5965.
(9) Ke, S.-H.; Yang, W.; Baranger, H. U. *Nano Lett.* **2008**, *8* (10), 3257−3261.
(10) Cardamone, D. M.; Stafford, C. A.; Mazumdar, S. *Nano Lett.* **2006**, *6* (11), 2422−2426.
(11) Markussen, T.; Stadler, R.; Thygesen, K. S. *Phys. Chem. Chem. Phys.* **2011**, *13* (32), 14311−14317.
(12) Ernzerhof, M. *J. Chem. Phys.* **2011**, *135* (1), 014104.
(13) Mayor, M.; Weber, H. B.; Reichert, J.; Elbing, M.; von Hanisch, C.; Beckmann, D.; Fischer, M. *Angew. Chem., Int Ed.* **2003**, *42* (47), 5834−5838.
(14) Taniguchi, M.; Tsutsui, M.; Mogi, R.; Sugawara, T.; Tsuji, Y.; Yoshizawa, K.; Kawai, T. *J. Am. Chem. Soc.* **2011**, *133* (30), 11426−11429.
(15) Fracasso, D.; Valkenier, H.; Hummelen, J. C.; Solomon, G. C.; Chiechi, R. C. *J. Am. Chem. Soc.* **2011**, *133* (24), 9556−9563.
(16) Xu, B. Q.; Xiao, X. Y.; Tao, N. J. *J. Am. Chem. Soc.* **2003**, *125* (52), 16164−16165.
(17) Frei, M.; Aradhya, S. V.; Koentopp, M.; Hybertsen, M. S.; Venkataraman, L. *Nano Lett.* **2011**, *11* (4), 1518−1523.
(18) Kamenetska, M.; Koentopp, M.; Whalley, A.; Park, Y.; Steigerwald, M.; Nuckolls, C.; Hybertsen, M.; Venkataraman, L. *Phys. Rev. Lett.* **2009**, *102* (12), 126803.
(19) Park, Y. S.; Whalley, A. C.; Kamenetska, M.; Steigerwald, M. L.; Hybertsen, M. S.; Nuckolls, C.; Venkataraman, L. *J. Am. Chem. Soc.* **2007**, *129* (51), 15768−15769.
(20) Rubio, G.; Agraït, N.; Vieira, S. *Phys. Rev. Lett.* **1996**, *76* (13), 2302−2305.
(21) Yanson, A. I.; Bollinger, G. R.; van den Brom, H. E.; Agrait, N.; van Ruitenbeek, J. M. *Nature* **1998**, *395* (6704), 783−785.
(22) Quek, S. Y.; Kamenetska, M.; Steigerwald, M. L.; Choi, H. J.; Louie, S. G.; Hybertsen, M. S.; Neaton, J. B.; Venkataraman, L. *Nat. Nanotechnol.* **2009**, *4* (4), 230−234.
(23) Park, Y. S.; Widawsky, J. R.; Kamenetska, M.; Steigerwald, M. L.; Hybertsen, M. S.; Nuckolls, C.; Venkataraman, L. *J. Am. Chem. Soc.* **2009**, *131* (31), 10820−10821.
(24) Meisner, J. S.; Kamenetska, M.; Krikorian, M.; Steigerwald, M. L.; Venkataraman, L.; Nuckolls, C. *Nano Lett.* **2011**, *11* (4), 1575−1579.
(25) Chen, F.; Hihath, J.; Huang, Z.; Li, X.; Tao, N. J. *Annu. Rev. Phys. Chem.* **2007**, *58*, 535−564.
(26) *Jaguar*, v7.8; Schrödinger, LLC: New York, 2011.
(27) King, B. T.; Kroulik, J.; Robertson, C. R.; Rempala, P.; Hilton, C. L.; Korinek, J. D.; Gortari, L. M. *J. Org. Chem.* **2007**, *72* (7), 2279−2288.
(28) Michinobu, T.; Boudon, C.; Gisselbrecht, J. P.; Seiler, P.; Frank, B.; Moonen, N. N. P.; Gross, M.; Diederich, F. *Chem.—Eur. J.* **2006**, *12* (7), 1889−1905.
(29) Hansch, C.; Leo, A.; Taft, R. W. *Chem. Rev.* **1991**, *91* (2), 165−195.
(30) Pauling, L. *The Nature of the Chemical Bond and the Structure of Molecules and Crystals: An Introduction to Modern Structural Chemistry*, 3rd ed.; Cornell University Press, Ithaca, NY, 1960.
(31) Mayor, M.; Buschel, M.; Fromm, K. M.; Lehn, J. M.; Daub, J. *Ann. N.Y. Acad. Sci.* **2002**, *960*, 16−28.